



**HAL**  
open science

## Fitting interatomic potentials consistent with thermodynamics: Fe, Cu, Ni and their alloys

Giovanni Bonny, Roberto C Pasianot, Lorenzo Malerba

► **To cite this version:**

Giovanni Bonny, Roberto C Pasianot, Lorenzo Malerba. Fitting interatomic potentials consistent with thermodynamics: Fe, Cu, Ni and their alloys. *Philosophical Magazine*, 2009, 89 (34-36), pp.3451-3464. 10.1080/14786430903299337 . hal-00541686

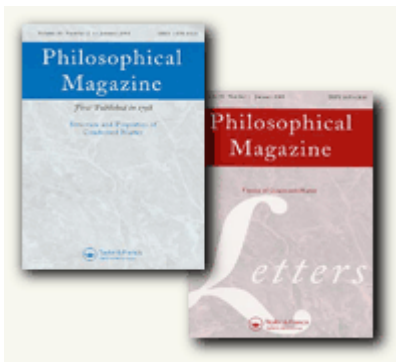
**HAL Id: hal-00541686**

**<https://hal.science/hal-00541686>**

Submitted on 1 Dec 2010

**HAL** is a multi-disciplinary open access archive for the deposit and dissemination of scientific research documents, whether they are published or not. The documents may come from teaching and research institutions in France or abroad, or from public or private research centers.

L'archive ouverte pluridisciplinaire **HAL**, est destinée au dépôt et à la diffusion de documents scientifiques de niveau recherche, publiés ou non, émanant des établissements d'enseignement et de recherche français ou étrangers, des laboratoires publics ou privés.



**Fitting interatomic potentials consistent with thermodynamics: Fe, Cu, Ni and their alloys**

Journal:	<i>Philosophical Magazine &amp; Philosophical Magazine Letters</i>
Manuscript ID:	TPHM-09-May-0229.R1
Journal Selection:	Philosophical Magazine
Date Submitted by the Author:	28-Aug-2009
Complete List of Authors:	Bonny, Giovanni; SCK-CEN, Nuclear Materials Science Institute Pasionot, Roberto; CAC-CNEA, Materials Department Malerba, Lorenzo; SCK-CEN, Nuclear Materials Science Institute
Keywords:	interatomic potential, phase diagrams, thermodynamics
Keywords (user supplied):	fitting techniques



# Fitting interatomic potentials consistent with thermodynamics: Fe, Cu, Ni and their alloys

G. Bonny<sup>1,2,\*</sup>, R.C. Pasianot<sup>3,4,5</sup> and L. Malerba<sup>1</sup>

<sup>1</sup> SCK•CEN, Nuclear Materials Science Institute, Boeretang 200, B-2400 Mol, Belgium

<sup>2</sup> Ghent University, Center for Molecular Modeling, Proeftuinstraat 86, B-9000 Gent, Belgium

<sup>3</sup> CAC-CNEA, Departamento de Materiales, Avda. Gral. Paz 1499, 1650 San Martín, Argentina

<sup>4</sup> CONICET, Avda. Rivadavia 1917, 1033 Buenos Aires, Argentina

<sup>5</sup> Instituto Sábató, UNSAM/CNEA, Avda. Gral. Paz 1499, 1650 San Martín, Argentina

## Abstract

In computational materials science, many atomistic methods hinge on an interatomic potential to describe the material properties. In alloys, besides a proper description of problem specific properties, a reasonable reproduction of the experimental phase diagram by the potential is essential. In this framework, we developed two complementary methods to fit interatomic potentials to the thermodynamic properties of the alloy. The first method involves the zero Kelvin phase diagram and makes use of the concept of the configuration polyhedron. The second method involves phase boundaries at finite temperature and is based on the cluster variation method. As an example for both techniques, they are applied to the Fe-Cu, Fe-Ni and Cu-Ni systems. The resulting potentials are compared to those found in the literature and are found to reproduce the experimental phase diagram more consistently than the latter.

## 1. Introduction

The use of atomistic simulation methods is becoming increasingly important in materials science. First principles methods, such as density functional theory (DFT), have proven to be very accurate tools in describing various materials properties. However, due to their inherent complexity, such schemes are only applicable to small scale atomic systems (typically  $<10^3$  atoms). When mechanical properties and micro-structure are the focus of attention,

1  
2 simulations have to be simple enough to deal with a large number of atoms (typically  $10^5$ - $10^7$   
3 atoms), thus capturing the length scale that is relevant for this class of problems. For such a  
4 purpose, classical short-ranged cohesive energy models remain an unavoidable constraint.  
5  
6

7 Historically, the first approach used to describe atomic interactions was by simple pair  
8 potentials. Although this scheme is suitable for rare-gas solids, it shows a number of  
9 deficiencies when applied to metals [1, 2]. The solution to these problems was the  
10 introduction of an additional many-body term, dependent on a variable describing the local  
11 atomic coordination (henceforth density). Based on different physical grounds, and  
12 independently from each other, three groups implemented such a scheme, namely, the “glue  
13 model” (GM) developed by Ercolessi *et al.* [3-5], the “embedded atom method” (EAM)  
14 developed by Daw and Baskes [6, 7] and the “Finnis-Sinclair” (FS) formalism developed by  
15 Finnis and Sinclair [1]. From a computational point of view, all three schemes are identical  
16 with a performance of the same order as simple pair potentials. In what follows we refer to the  
17 three formalisms as many-body central force potentials. In the literature, several extensions  
18 based on many-body central force potentials exist, introducing for example bond-angle  
19 dependences [8-11] or local concentration dependences [12, 13]. For most transition metals  
20 and their alloys, however, many-body central force potentials are still widely used.  
21  
22

23 In the literature, a number of many-body central force potentials are available for pure  
24 elements (see for example [14-17]) and, especially in the last few years, also multi-component  
25 potentials (mostly binary) have been developed (see for example [14, 18-21]). In most cases,  
26 besides problem-specific properties (e.g. point defect interaction energies and their migration  
27 barriers), the mixing enthalpy at low temperature (0 K for DFT data) and/or formation energy  
28 of some intermetallic compounds is the only thermodynamic information included in the fit.  
29 Such approaches are currently considered “common practice” (see for example [11, 22-25])  
30 and are also applied to the potentials fitted here. The mixing enthalpy determines the alloy's  
31 thermodynamics in the high temperature limit, and can thus be a sufficient description for  
32 disordered alloys. The formation energy of intermetallic compounds, on the other hand, gives  
33 the absolute stability of the compound, but can hardly control the stabilization of other  
34 (unphysical) compounds. It is thus clear that, for many alloys of technological interest, a fit to  
35 the mixing enthalpy or formation energy of some intermetallic compounds does not suffice,  
36 and that more elaborate methods to fit thermodynamic information is necessary.  
37  
38

39 In this paper we develop two methods to account for the experimental phase stabilities.  
40 The first method, based on the probability polyhedron [26, 27], aims at controlling the  
41  
42  
43  
44  
45  
46  
47  
48  
49  
50  
51  
52  
53  
54  
55  
56  
57  
58  
59  
60

---

\* Corresponding author, email: gbonny@sckcen.be

1  
2 allowable ground states. This method is of particular interest when intermetallic compounds  
3 appear in the phase diagram. The second method is based on the cluster variation method  
4 (CVM) [28] and aims at fitting the experimental solid phase boundaries at finite temperature.  
5  
6

7 As an illustration of the performance of both methods, they are applied to the Fe-Cu,  
8 Fe-Ni and Cu-Ni binary systems, which together form a ternary Fe-Cu-Ni potential. The Fe-  
9 Cu and Fe-Cu-Ni systems are model alloys for reactor pressure vessel (RPV) steels.  
10 Experimentally it is known that nano-metric Cu-rich precipitates cause hardening and  
11 embrittlement in such steels [29-38]. It is thus essential that the potential closely reproduces  
12 the Cu solubility, a demand handled with our second technique above. The Fe-Ni system,  
13 developed as a part of the ternary Fe-Cu-Ni system, on the other hand, also serves as a model  
14 alloy for austenitic steels, as used for example in current reactor's internal components.  
15 Experimentally, this system consists of a ferritic Fe rich phase, an austenitic Ni rich phase  
16 and, in-between, two fcc based  $L1_0$  FeNi and  $L1_2$  FeNi<sub>3</sub> intermetallic phases [39]. Here it is  
17 thus essential to correctly reproduce the stability of observed intermetallic phases, a demand  
18 handled with our first technique. The Cu-Ni potential on the other hand is a by-product of our  
19 ternary Fe-Cu-Ni potential, but for reasons of consistency it was also fitted to the  
20 experimental phase diagram. The phase diagram consists of a miscibility gap of two austenitic  
21 phases with total miscibility above a critical temperature [40-43]. As a first approximation  
22 this alloy can be considered disordered, and therefore we use it as an illustration of a case in  
23 which fitting to the mixing enthalpy only gives already a reasonable result.  
24  
25  
26  
27  
28  
29  
30  
31  
32  
33  
34  
35  
36

37 All of the above potentials were fitted to many other properties (mostly defect  
38 properties), besides thermodynamic data. As an illustration of the methods, however, here we  
39 only present the thermodynamic aspects and compare them against experiments and other  
40 potentials found in the literature. For more details on the other properties, the reader is  
41 referred to [20, 21, 44]. To conclude, a closing discussion on the applicability and limitations  
42 of the developed fitting techniques is given.  
43  
44  
45  
46  
47  
48  
49

## 50 2. Potential formalism

51  
52 For the sake of definiteness, the interactions are expressed using the EAM scheme. We note,  
53 however, that the fitting techniques are not restricted to this formalism and can in fact be  
54 applied using other ones, including bond-angle dependent and concentration dependent  
55 formalisms. Within EAM, in addition to a pair interaction term,  $V$ , a so-called embedding  
56 term,  $F$ , dependent on the electron density  $\rho$ , is included. The latter contribution  
57  
58  
59  
60

approximates the many-body interaction with the surrounding neighbours. The total energy is thus given as,

$$E = \frac{1}{2} \sum_{\substack{i,j=1 \\ j \neq i}}^N V_{t_i t_j}(r_{ij}) + \sum_{i=1}^N F_{t_i}(r_i). \quad (1)$$

Here  $N$  represents the total number of atoms in the system,  $r_{ij}$  is the distance between atoms  $i$  and  $j$ , and  $t_i$  denote atomic species. The electron density around atom  $i$ , contributed from its neighbours is in turn given as,

$$r_i = \sum_{\substack{j=1 \\ j \neq i}}^N j_{t_j}(r_{ij}), \quad (2)$$

where  $\varphi$  denotes the electron density function of the considered element. The form of  $V$ ,  $F$  and  $\varphi$  is, however, not uniquely determined. Two transformations [1, 2, 18],  $\hat{T}_1$  and  $\hat{T}_2$ , exist that leave the total energy invariant,

$$\hat{T}_1 \begin{matrix} j \\ \vdots \\ j \\ \vdots \\ F(r) \end{matrix} \otimes \begin{matrix} S \\ \vdots \\ S \\ \vdots \\ F(r/S) \end{matrix} \quad (3)$$

$$\hat{T}_2 \begin{matrix} F(r) \\ \vdots \\ F(r) \\ \vdots \\ V(r) \end{matrix} \otimes \begin{matrix} F(r) + C \\ \vdots \\ F(r) + C \\ \vdots \\ V(r) - 2Cj(r) \end{matrix}, \quad (4)$$

with  $C$  and  $S$  arbitrary constants. Therefore, the units of the electron density are arbitrary for the pure species, but contribute to each other's embedding energy in the alloy case.

In what follows, we assume that the potentials for the pure species are given, and only the cross pair interactions  $V_{AB}$  and relative weight between the electron densities  $\rho_A/\rho_B$  need to be determined. During the fitting of the alloy properties, transformation  $\hat{T}_1$  is used to change the relative weight between the electron densities  $\rho_A/\rho_B$ . The mixed pair interaction  $V_{AB}$ , on the other hand, is parameterized by the spline expansion,

$$V(r_{ij}) = \sum_{k=1}^{N_p} a_k (r_k - r)^3 H(r_k - r), \quad (5)$$

where  $N_p$  denotes the number of knots,  $a_k$  are the fitting parameters and  $H$  denotes the Heaviside unit step function.

### 3. Fitting procedure

The fitting of an interatomic potential can be viewed as a problem of finding the potential parameters that allow the latter to optimally reproduce a given data set, presently, thermodynamic data. Mathematically, it can be formulated as the minimization of the overall squared deviation, so called objective function (OF), between predicted and reference data, possibly including some constraints. Simple thermodynamic properties, such as the random mixing enthalpy, or formation energy of intermetallic compounds, are relatively easy to express. Moreover, if relaxation effects can be neglected, Equation (5) leads essentially to a quadratic programming problem [45] to determine the parameter set  $\{a_k\}$ . Otherwise, if relaxation effects matter, the intermetallic compound structures need first to be relaxed for each trial parameter set, thereby leading to nested optimizations. In the same context, for mimicking the random alloy, one may use relatively small so-called special quasi-random structures (SQSs) [46]. Thus, more elaborate minimization routines would be necessary. The two fitting techniques proposed below are of the latter kind; it will also be shown that relaxations are not the only cause of complexity in the optimization procedure.

#### 3.1. Ground States

At low temperature, the phase diagram is determined by the static properties of the alloy. For disordered alloys this is the random mixing enthalpy while for intermetallic phases this is the formation energy of intermetallic compounds. In the absence of intermetallic compounds a fit to the random mixing enthalpy can be sufficient to describe randomly disordered alloys, but for alloys governed by intermetallic phases a more elaborate approach is necessary. Besides fitting the formation energy of the intermetallic compounds of interest, constraints must be applied to control the relative stability with respect to other possible intermetallic compounds. Such a procedure is necessary to guarantee that the compounds of interest are the **only** ground states of the system, so that no unwanted (unphysical) phases appear in the phase diagram. On

the other hand, if no intermetallics should be expected, such constraints are used to ensure that no intermetallic compounds are stabilized by the potential.

For a binary alloy with a given lattice symmetry, there exist  $\sum_{n=1}^M 2^n$  possible ordered compounds for a unit cell containing up to  $M$  atoms. These ordered compounds can easily be enumerated as described in [47], but it is clear that the total number of compounds increases fast with  $M$ , among which only a selected few represent possible ground states of the system under investigation. It is thus desirable to sample only the compounds that are candidate ground states rather than enumerating all. A way to perform this is based on the configuration polyhedron [26, 27]. In short, given a lattice and a (set of) maximal clusters upon it, the configuration polyhedron is a convex region in the correlation functions (CF) space where the probability of any specified cluster configuration is assured to be non-negative (c.f. next section for further details). Since the configurational energy on a rigid lattice can be written as a linear cluster expansion in CF space [26, 27, 48], the vertices of such a polyhedron are candidates to system's ground states, though not all of the associated ordered compounds are feasible, i.e., physically possible for the given lattice. In what follows we understand this concept in the latter more restricted sense of feasible vertices, denoting also the  $m^{\text{th}}$  CF for a cluster comprising  $n$  sites as  $\zeta_{n,m}$ .

Finel [49] studied the bcc lattice by using two maximal clusters, the standard octahedron and the cubic unit cell, so distances up to 5th nearest neighbour (5nn) were considered, except 4nn. In that work a polyhedron of 28 vertices (with 97 faces in the 5-D space spanned by the CFs  $\zeta_1$ ,  $\zeta_{2,1}$ ,  $\zeta_{2,2}$ ,  $\zeta_{2,3}$  and  $\zeta_{2,5}$ ) was constructed and the vertices were identified with the associated ordered compounds. We have enlarged this polyhedron by selecting ordered compounds from previous ATAT [50, 51] runs, used to construct the Fe-Cu phase diagram [20]. For each of these compounds the respective CFs were determined in 6-D space spanned by the point correlation function  $\zeta_1$  and five doublets up to 5nn:  $\zeta_{2,1}, \zeta_{2,2}, \zeta_{2,3}, \zeta_{2,4}$  and  $\zeta_{2,5}$ . Then these CFs were checked for convexity against the 28 original vertices given by Finel, with the result that the number of vertices of the polyhedron was raised to 99 (with 1750 faces in 6-D space). The ordered compounds corresponding to these vertices are referred to as BCC-99 and serve to sample possible ground states.

Similarly, Kanamori and Kakehashi [52] studied the fcc lattice using a different method from Finel's, and reported a set of 87 ordered compounds, referred to as FCC-87, relevant to interactions up to 4nn (although they do not exhaust all the possibilities according to Finel [49]). It was checked that they can be taken as vertices of a polyhedron possessing 691 faces

in the 6-D space spanned by the point and the doublets up to 5nn (174 if up to 4nn, but then 14 compounds lay on the boundary without being vertices; they are numbers 2,4,27,28,32,36 and 37 (and the complementary ones) of reference [52]).

Given the compounds corresponding to the BCC-99 and FCC-87, we impose by constraints that the formation energy of all of them for a trial potential should lay above the convex hull of formation energies of the experimentally observed intermetallic compounds. This procedure leads thus to 186 constraints during the optimisation of the potential parameters.

### 3.2. Phase boundaries at finite temperature

The main problem of fitting a potential to the experimental phase diagram at finite temperature is precisely the evaluation of the phase diagram corresponding to the trial potential. In the literature, many Monte Carlo and molecular dynamics based algorithms are available to compute the solid state phase diagram for a given potential [51, 53-56], but their computation time is prohibitive for their use during potential fitting. An alternative, computationally feasible procedure to estimate the solid state phase diagram is to use CVM to obtain the free energy together with the common tangent method [57] to track the phase boundaries.

According to general statistical mechanics principles, free energies can be expressed as variational problems in a configuration (site occupation) space [26, 27]. Particularly, for rigid periodic lattices the Helmholtz free energy per site,  $f(T,c)$ , may be written as,

$$f = \min_x \sum_{a \in \alpha_M} \hat{a} m_a E_a x_a + k_B T \sum_{a \in \alpha_M} \hat{a} m_a a_a \sum_s \hat{a}_s p_a(s) \ln p_a(s), \quad (6)$$

where the first term represents the internal energy and the second one embodies the configurational entropy. The outer sums extend over the symmetry-equivalent clusters of sites, that are subsets of a (family of) chosen maximal ones,  $\alpha_M$ . The multiplicity of these clusters is  $m_\alpha$ ;  $a_\alpha$  are coefficients related to crystal symmetry and computed within the framework of the CVM theory;  $p_\alpha$  are cluster probability distribution functions depending on the system configuration  $\sigma$ ; the variational parameters,  $\xi = \{\xi_\alpha\}$ , i.e. CFs, are in turn linearly related to  $p_\alpha$ ; finally,  $E_\alpha$  are the coefficients of the energy expansion upon the cluster basis

used, thus carrying the specific interaction model. Regarding the entropy term, many calculations of phase diagrams using the CVM have been performed with relatively small  $\alpha_M$  clusters, which nevertheless were able to obtain rather non trivial phase diagram structures. These are mainly the tetrahedron-octahedron approximation for the fcc lattices, and the tetrahedron approximation for the bcc ones, which are used here in their expressions for disordered alloys [26, 27]. The minimization in Equation (6) is constrained to a convex region in CF space where  $0 \leq p_a \leq 1$ , which is the configuration polyhedron as presented above.

Once the free energy is obtained, the experimental solubility limits  $x_\alpha$  and  $x_\beta$  for the phases  $\alpha$  and  $\beta$ , respectively, at a given temperature  $T$ , are fitted through the common tangent equations,

$$\begin{cases} f_a - x_a f'_a = f_b - x_b f'_b \\ f_a + x_b f'_a = f_b + x_a f'_b \end{cases} \quad (7)$$

Here  $f_\alpha$  is the free energy per atom at temperature  $T$  for concentration  $x_\alpha$ , and  $f'_\alpha$  represents the derivative with respect to  $x$  taken in the point  $x_\alpha$  (and similar for the  $\beta$ -phase). This procedure can be applied to fit as many experimental phase boundary points as wished.

The constrained minimization in Equation (6) with respect to  $\xi$  is complicated because, (i) each face of the configuration polyhedron introduces an inequality constraint; (ii) the cluster expansion for the energy may require more  $\xi_\alpha$  than required for the CVM entropy (leading to instabilities in the resulting free energy). Although approximate solutions exist for the latter [58], for large configuration polyhedrons, as is the case here, the minimization is unmanageable.

A technique that largely overcomes these problems reverts to the so called barycentric coordinates, namely, each point within the CF polyhedron can be expressed as,

$$\xi = \sum_i \lambda_i \mathbf{V}_i, \quad (8)$$

where  $\mathbf{V}_i = \{V_i^{(1)}, \dots, V_i^{(n,m)}\}$  are the coordinates (vector in CF space) for each vertex  $i$  of the configuration polyhedron. The barycentric coordinates,  $\lambda_i$  (99 for the bcc lattice and 87 for the fcc one) comply to the relations,

$$l_i \geq 0 \text{ and } \sum_i l_i = 1. \quad (9)$$

Such a representation is generally non unique, but this is inconsequential for our purposes. Notice that  $\mathbf{V}_i$  can be determined up to the number of dimensions desired from the associated intermetallic compound.

The barycentric coordinates are a very convenient tool to handle CFs, in fact, the latter are strictly needed only to express the entropy within the CVM approach, not the energy. First, it is important to realize that the positive combination of Equation (8) represents a positive combination of feasible probability distribution functions, and thus also a new feasible probability distribution function. Second, because the vertices themselves can include as many CFs as needed to cluster expand the energy, the latter is given by the same linear combination of vertex energies for any point belonging to the polyhedron. Therefore, the energy can also be expanded as,

$$E(\xi) = \sum_i l_i E_i. \quad (10)$$

Here  $E_i$  is the energy of compound corresponding to vertex  $\mathbf{V}_i$ , that was optimised using the trial potential. Also, constraints on the barycentric coordinates, Equation (9), are easier to implement than on CFs, and their meaning is more transparent due to the direct relationship to individual compounds. In summary, the use of barycentric coordinates makes the minimization more stable and the resulting free energy more reliable.

## 4. Applications

### 4.1. Iron-nickel model alloy

In this section we take our Fe-Ni potential from [21] to illustrate the importance of applying the first of the above described fitting techniques. This fact is highlighted by comparing with two potentials found in the literature. The first one was developed by Meyer and Entel [59] in the EAM formalism for the purpose of studying the austenite-martensite transformation by varying Ni content and employing MD techniques. The second potential, by Mishin *et al.* [11], was developed mainly to study the phase stability of ordered  $\text{Fe}_{1-x}\text{Ni}_x$  compounds, and

1  
2  
3  
4  
5  
6  
7  
8  
9  
10  
11  
12  
13  
14  
15  
16  
17  
18  
19  
20  
21  
22  
23  
24  
25  
26  
27  
28  
29  
30  
31  
32  
33  
34  
35  
36  
37  
38  
39  
40  
41  
42  
43  
44  
45  
46  
47  
48  
49  
50  
51  
52  
53  
54  
55  
56  
57  
58  
59  
60

is based on the, so called, angle dependent potential (ADP) formalism [11]. The latter is an extension of EAM, but includes bond-angle contributions, that in principle allow for a more accurate fitting to DFT data available on intermetallic compounds. In what follows the two potentials are referred to as MEY and MISH, respectively.

In Figure 1 the lowest energies of the BCC-99 and FCC-87 compounds, computed with the three different potentials are compared. The figure clearly shows the importance of the constraints on the possible intermetallic compounds introduced in the fitting procedure. For the MISH potential, as already reported [11], the formation energy of the compounds  $C11_f$  at 33.33 and 66.67 at.% Ni lay on and just above the hull, respectively, while the compound at 88.75 at.% Ni (  $Ca_7Ge$  type ) lays below the hull and thus represents an (unwanted) ground state of the system. Note also that the examination of the BCC-99 and FCC-87 structures reveals the existence of many other ordered compounds, especially between 50 and 100 at.% Ni, with a formation energy only a few meV above the convex hull of truly ground states. These are metastable states that could become of importance at finite temperature. Turning to the MEY potential, it appears that the experimentally observed intermetallics  $L1_0$  FeNi and  $L1_2$  FeNi<sub>3</sub> are not even ground states of the system. As shown in the figure, the phase diagram consists in this case of over ten compounds, none of which is  $L1_0$  FeNi or  $L1_2$  FeNi<sub>3</sub>. In summary, we see that the here fitted potential is the only one capable of reproducing the experimental phase diagram at 0 K, being at the same time derived within the relatively simple EAM formalism, thanks to the application of the fitting procedure described in Section 3.1.

#### 4.2. Iron-copper model alloy

Our Fe-Cu potential published in [20] provides an example of application of the second of the above-described fitting techniques. The thermodynamic reliability of the potential is here contrasted to experimental data and to similar results obtained with two potentials from the literature. The first of these was developed by Ackland *et al.* [60] using the FS formalism to study point defect properties in low Cu ferritic RPV steels. The second one was developed by Ludwig *et al.* [61] in the EAM formalism to study the interface between Cu precipitates and the Fe matrix, as well as their effect on the dislocation core structure. In what follows they are referred to as ACK and LUD, respectively.

Figure 2 shows the Cu solubility in Fe obtained from all three potentials. The curves for both ACK and LUD are taken from [62] and [63], respectively. The phase boundaries

1  
2 obtained in these works are based on a full thermodynamic integration accounting for all  
3 components in the free energy. In the case of our potential, however, the vibrational entropy  
4 was verified to be negligible and was consequently not included in the phase diagram  
5 computation. The experimental data from Salje and Feller-Kniepmeier [64] and from Perez *et*  
6 *al.* [65] are also included in the figure. The former were obtained from the diffusion profile  
7 measurements of a thin Cu deposit onto an Fe substrate. The latter were obtained from  
8 thermoelectric power and small angle X-ray scattering measurements in thermally aged Fe-Cu  
9 alloys, where Cu precipitation was thereby induced. In fact, the latter points correspond to  
10 equation (10) from Ref. [65] evaluated at the measuring temperatures. Clearly, our potential  
11 follows the experimental results very well, perhaps with a little over/under-estimated  
12 solubilities for temperatures below/above 1000 K. The other two potentials, on the other hand,  
13 give too high solubility, particularly ACK. In summary, we see that the here fitted potential  
14 obtains a better fit to the experimental phase boundary at all temperatures, than if only the  
15 mixing energies at 0 K were used as data to be fitted.  
16  
17  
18  
19  
20  
21  
22  
23  
24  
25  
26  
27  
28

#### 29 4.3. Copper-nickel model alloy

30  
31  
32 Our Cu-Ni potential, on which further details can be found in [44], provides an example of  
33 potential fitted to the random solution mixing enthalpy only. The phase diagram predicted by  
34 our potential is compared to Calphad calculated data [66] and to the phase diagram from two  
35 potentials found in the literature. The first of these potentials was developed by Asta *et al.*  
36 [23] in the EAM formalism. The authors studied the structural and thermodynamic properties  
37 of solid solutions using a computational approach which combines the EAM description of  
38 alloy energetics with a second-order-expansion treatment of compositional and displacive  
39 disorder. The second potential is the work of Lee and Shim [25] and uses the modified  
40 embedded atom method (MEAM). It was developed to comply with the basic thermodynamic  
41 properties of Cu-Ni. The latter potential was quoted to be a part of a long term project to  
42 construct a ternary Fe-Cu-Ni potential to investigate the primary damage defect creation in  
43 RPV steels, although to date the ternary Fe-Cu-Ni potentials remains unpublished to our  
44 knowledge. In what follows, these two potentials are referred to as AST and LEE,  
45 respectively.  
46  
47  
48  
49  
50  
51  
52  
53  
54  
55  
56

57 In Figure 3 the miscibility gap calculated for all three potentials is compared with the  
58 most recent Calphad parameterizations [42, 43]. The miscibility gap predicted by both the  
59 AST and LEE potential were taken from [23] and [25], respectively, which claim to account  
60

1  
2 for all components in the free energy. In the case of our potential, the vibrational entropy was  
3 verified to be negligible and was consequently not included in the phase diagram  
4 computation. Prior to comparing the miscibility gaps obtained from the potentials with each  
5 other and with the Calphad computed phase diagrams, a comment regarding the uncertainties  
6 in the latter is necessary. Experimentally, the existence of a Cu-Ni miscibility gap has been  
7 confirmed. However, disagreement exists regarding its composition and temperature range, so  
8 the corresponding Calphad phase diagram is mostly based on (speculative) thermodynamic  
9 calculations (see [42] and references therein). Therefore, the Calphad curves should be taken  
10 here as indicative curves, rather than experimentally verified phase boundaries. Taking this  
11 comment into account, the agreement of the miscibility gaps computed from all potentials is  
12 in reasonable agreement with the Calphad parameterizations. The asymmetry in the  
13 miscibility gap, however, is only reproduced by the AST potential, while the miscibility gaps  
14 resulting from our potential and LEE exhibit the opposite and no symmetry, respectively.

15  
16 Thus, in this case, where no special care was taken to reproduce specific structure  
17 stability or phase diagram boundary, our potential performs similarly to existing ones. It  
18 should be noted, that the relative weight of the electron densities  $\rho_{\text{Cu}}/\rho_{\text{Ni}}$  in our potential was  
19 already fixed during the fitting of the Fe-Ni and Fe-Cu potentials. Allowing for this weight to  
20 change and applying our second fitting technique, the correct asymmetry and a closer fit to  
21 one of the Calphad calculated miscibility gaps could be obtained. This would be, however, at  
22 the cost of compatibility with the Fe-Ni and Fe-Cu potentials. Thus, for reasons of  
23 compatibility and in view of the experimental uncertainties, we opted to fix  $\rho_{\text{Cu}}/\rho_{\text{Ni}}$  as  
24 determined by the Fe-Ni and Fe-Cu binaries so that all three binaries together form a ternary  
25 EAM potential.

## 26 27 28 29 30 31 32 33 34 35 36 37 38 39 40 41 42 43 44 45 46 47 48 49 50 51 52 53 54 55 56 57 58 59 60

### 5. Discussion

Both methods presented above are generally applicable to a wide range of systems. In some cases, however, the peculiarities of the system make our techniques unsuitable. An example of this is the Fe-Cr system, that may exhibit intermetallic compounds, and certainly exhibits short-range order in the Fe-rich limit, i.e. <10 at.% Cr [67-69]. The BCC-99 (and also FCC-87) compounds presented above do not exhaust unit cells larger than about nine atoms. In principle, this problem can be solved by increasing the unit cell size to describe a concentration range below 10 at.% Cr. In practice, however, such a probability polyhedron (in 6-D) will consist of over 10,000 vertices, which are all constraints to be accounted for in the

1  
2 potential and CVM optimization. Moreover, many physically different structures would be  
3 degenerate within our current 6-D coordinates, thus leading to the need of non-pair  
4 coordinates, and possibly, for consistency reasons, to more complicated (and untested)  
5 expressions of the CVM entropy. Clearly, this greater complexity and prohibitive high  
6 number of constraints limits the method's applicability. In particular, systems exhibiting  
7 intermetallic compounds in their dilute limits may not be handled.  
8

9  
10  
11  
12 For all three example systems, information regarding the random mixing enthalpy was  
13 included in the fit. Currently, this is performed by a mean field expansion of the mixing  
14 enthalpy as a function of composition [70] that neglects relaxations. Such a strategy proved  
15 sufficiently accurate, but for systems where relaxation effects are an issue, SQSs can be used  
16 to mimick the randomly disordered alloys. These structures in turn can be optimized in the  
17 same way as the BCC-99 and FCC-87 compounds. Also, for none of the current systems  
18 vibrational entropy was considered. If necessary, however, the method is easily extendable to  
19 fit vibrational entropy. Once the relaxed structure of an SQS, BCC-99 or FCC-87 compound  
20 is obtained, the Hessian matrix is calculated, from where the vibrational entropy in the  
21 harmonic approximation [71] can be obtained. With these remarks, we cover the most  
22 important aspects to included when fitting many-body potentials consistent with  
23 thermodynamics.  
24

25  
26  
27 To finalize, it is worth emphasizing that the application of both our proposed techniques  
28 (and possible extensions) require optimizers able to work with function values only, of  
29 unknown or even ill defined derivatives. Firstly, SQSs and/or the compounds associated with  
30 the BCC-99 or FCC-87 polyhedrons are optimized for each trial parameter set  $\{a_k\}$ , then the  
31 latter is varied to optimize the OF, thus introducing a nested minimization. When applying the  
32 second method, still an additional constrained minimization with respect to correlation  
33 functions is necessary to obtain the free energy. Among the optimizers available in the  
34 literature, we found the (freely available) deterministic one by Powell [72] (COBYLA) to be a  
35 good compromise between computation time and quality of results.  
36  
37

## 38 39 40 41 42 43 44 45 46 47 48 49 50 51 52 **6. Summary and conclusions**

53  
54  
55 We have presented and described in some detail two advanced methods to fit the  
56 thermodynamic properties of alloys when developing classical interatomic potentials. The  
57 first method involves the zero Kelvin phase diagram and uses the configuration polyhedron. It  
58 is especially suitable to fit potentials that reproduce experimentally observed intermetallic  
59  
60

1  
2 phases. The second method involves the phase boundaries at finite temperature and is based  
3 on the cluster variation method. It is especially suitable to closely reproduce the experimental  
4 phase boundaries.  
5  
6

7 Both methods were successfully applied to the Fe-Cu, Fe-Ni and Cu-Ni systems that  
8 together form a ternary Fe-Cu-Ni potential. It was shown that all potentials reasonably agree  
9 with the experimental phase diagram and equally (Cu-Ni case) or more consistently (when the  
10 presented procedures are used) with experiments than recent potentials found in the literature.  
11  
12  
13  
14

### 15 16 **Acknowledgements**

17  
18  
19  
20 This work was performed in the framework of the FP6/PERFECT project, partially supported  
21 by the European Commission (EC), under contract FI60-CT-2003-5088-40. It also contributes  
22 to the EC funded FP7/PERFORM60 project, grant agreement 232612. The work was also  
23 sponsored by the SECYT-FWO bilateral cooperation agreement, Project FW/07/EXII/002.  
24  
25 RCP wishes to acknowledge partial support from CONICET-PIP 5062.  
26  
27  
28  
29

### 30 31 **References**

- 32  
33  
34 [1] M.W. Finnis and J.E. Sinclair, *Phil. Mag. A* 50 (1984) p. 45.  
35 [2] F. Ercolessi, M. Parrinello and E. Tosatti, *Phil. Mag. A* 58 (1988) p. 213.  
36 [3] F. Ercolessi, PhD thesis, University of Trieste, 1983.  
37 [4] M. Garofalo, Thesis, International School for Advanced Studies, Trieste, 1984.  
38 [5] F. Ercolessi, E. Tosatti and M. Parrinello, *Phys. Rev. Lett.* 57 (1986) p. 719.  
39 [6] M.S. Daw and M.I. Baskes, *Phys. Rev. Lett.* 50 (1983) p. 1285.  
40 [7] M.S. Daw and M.I. Baskes, *Phys. Rev. B* 29 (1984) p. 6443.  
41 [8] M.I. Baskes, *Phys. Rev. Lett.* 59 (1987) p. 2666.  
42 [9] M.I. Baskes, *Phys. Rev. B* 46 (1992) p. 2727.  
43 [10] R. Pasianot, D. Farkas and E.J. Savino, *Phys. Rev. B* 43 (1991) p. 6952.  
44 [11] Y. Mishin, M.J. Mehl and D.A. Papaconstantopoulos, *Acta Mater.* 53 (2005) p. 4029.  
45 [12] P. Olsson, J. Wallenius, C. Domain, K. Nordlund and L. Malerba, *Phys. Rev. B* 72  
46 (2005) p. 214119.  
47 [13] A. Caro, D.A. Crowson and M. Caro, *Phys. Rev. Lett.* 95 (2005) p. 75702.  
48 [14] S.M. Foiles, M.I. Baskes and M.S. Daw, *Phys. Rev. B* 33 (1986) p. 7983.  
49  
50  
51  
52  
53  
54  
55  
56  
57  
58  
59  
60

- 1  
2 [15] *Intermetallic Compounds: Principles*, Volume 1, Eds J.H. Westbrook and R.L. Fleischer,  
3 John Wiley & Sons, 1994.  
4  
5 [16] Y. Mishin, D. Farkas, M.J. Mehl and D.A. Papaconstantopoulos, *Phys. Rev. B* 59 (1999)  
6 p. 3393.  
7  
8 [17] M.I. Mendeleev, A. Han, D.J. Srolovitz, G.J. Ackland, D.Y. Sun and M. Asta, *Phil. Mag.*  
9 *A* 83 (2003) p. 3977.  
10  
11 [18] R.A. Johnson and D.J. Oh, *J. Mater. Res.* 4 (1989) p. 1195.  
12  
13 [19] G.J. Ackland, M.I. Mendeleev, D.J. Srolovitz, S. Han and A.V. Barashev, *J. Phys.*  
14 *Condens. Mat.* 16 (2004) p. 1.  
15  
16 [20] R.C. Pasianot and L. Malerba, *J. Nucl. Mater.* 360 (2007) p. 118.  
17  
18 [21] G. Bonny, R.C. Pasianot and L. Malerba, *Model. Simul. Eng. Mater. Sci.* 17 (2009) p.  
19 025010.  
20  
21 [22] O. Yifang, Z. Bangwei, L. Shuzhi and J. Zhanpeng, *Z. Phys. B* 101 (1996) p. 161.  
22  
23 [23] M. Asta and S.M. Foiles, *Phys. Rev. B* 53 (1996) p. 2389.  
24  
25 [24] B.-J. Lee, J.-H. Shim and H.M. Park, *CALPHAD* 25 (2001) p. 527.  
26  
27 [25] B.-J. Lee and J.-H. Shim, *CALPHAD* 28 (2004) p. 125.  
28  
29 [26] F. Ducastelle, *Order and phase stability in alloys*, North-Holland, Amsterdam, 1991.  
30  
31 [27] G. Inden and W. Pitsch, *Phase Transformations in Materials*, Eds R.W. Cahn *et al.*,  
32 Wiley, Weinheim, 1991, p. 497.  
33  
34 [28] R. Kikuchi, *Phys. Rev.* 81 (1951) p. 988.  
35  
36 [29] U. Potapovs and J.R. Hawthorne, *Nucl. Appl.* 1 (1969) p. 27.  
37  
38 [30] G. Odette, *Scr. Metall.* 17 (1983) p. 1183.  
39  
40 [31] W. Phythian, C. English, *J. Nucl. Mater.* 205 (1993) p. 162.  
41  
42 [32] P. Auger, P. Pareige, A. Akamatsu, D. Blavette, *J. Nucl. Mater.* 225 (1995) p. 225.  
43  
44 [33] J.T. Buswell, W.J. Phythian, R.J. McElroy, S. Dumbill, P.H.N. Ray, J. Mace and R.N.  
45 Sinclair, *J. Nucl. Mater.* 225 (1995) p. 196.  
46  
47 [34] C. English, W. Phythian, R. McElroy, *Mater. Res. Soc. Symp. Proc.*, vol. 439, MRS,  
48 Pittsburgh, Pennsylvania, 1997, p. 471.  
49  
50 [35] G.R. Odette and G.E. Lucas, *JOM* 53 (2001) p. 18.  
51  
52 [36] Y. Nagai, Z. Tang, M. Hasegawa, T. Kanai, M. Saneyasu, *Phys. Rev. B* 63 (2001) p.  
53 134110.  
54  
55 [37] K. Morita, S. Ishino, T. Tobita, Y. Chimi, N. Ishikawa, A. Iwase, *J. Nucl. Mater.* 304  
56 (2002) p. 153.  
57  
58 [38] R. Chaouadi, R. Gerard, *J. Nucl. Mater.* 345 (2005) p. 65.  
59  
60

- 1  
2 [39] A.H. Reed, Metall. Mater. Trans. A 34 (2003) p. 1759.  
3  
4 [40] R.C. Sharma, Trans. Indian Inst. Met. 35 (1982) p. 372.  
5  
6 [41] S. Mey, Z. Metallkde. 78 (1987) p. 502.  
7  
8 [42] S. Srikanth and K.T. Jacob, Mater. Sci. Technol. 5 (1989) p. 427.  
9  
10 [43] S. Mey, CALPHAD 16 (1992) p. 255.  
11 [44] G. Bonny, R.C. Pasianot, N. Castin and L. Malerba, "Ternary Fe-Cu-Ni many-body  
12 potential to model reactor pressure vessel steels: First validation by simulated thermal  
13 annealing", submitted to Phil. Mag. (2009).  
14  
15 [45] J. Nocedal and S.J. Wright, *Numerical Optimization*, Springer-Verlag, New York, 2006,  
16 p. 449.  
17  
18 [46] A. Zunger, S.H. Wei, L.G. Ferreira and J.E. Bernard, Phys. Rev. Lett. 65 (1990) p. 353.  
19  
20 [47] L.G. Ferreira, S.-H. Wei, A. Zunger, Int. J. Supercomput. 5 (1991) p. 34.  
21  
22 [48] J.M. Sanchez, F. Ducastelle and D. Gratias, Physica A 128 (1984) p. 334.  
23  
24 [49] A. Finel, PhD thesis, Université Pierre et Marie Curie, Paris (1987).  
25  
26 [50] A. van de Walle, G. Ceder, J. Phase Equilibria 23 (2002) p. 348.  
27  
28 [51] A. van de Walle, M. Asta, Modelling Simul. Mater. Sci. Eng. 10 (2002) p. 521.  
29  
30 [52] J. Kanamori and Y. Kakehashi, J. Physique Coll. 38 (C7) (1977) p. 274.  
31  
32 [53] F.M. Marquez, C. Cienfuegos, B.K. Pongsai, M.Yu. Lavrentiev, N.L. Allan, J.A. Purton  
33 and G.D. Barrera, Modelling Simul. Mater. Sci. Eng. 11 (2003) p. 115.  
34  
35 [54] D. Frenkel and B. Smit, *Understanding Molecular Simulation – From Algorithms to*  
36 *Applications*, Academic, London, 1996.  
37  
38 [55] E. Agando Arregui, M. Caro and A. Caro, Phys. Rev. B 66 (2002) p. 054201.  
39  
40 [56] G. Bonny, P. Erhart, A. Caro, R.C. Pasianot, L. Malerba and M. Caro, Modelling Simul.  
41 Mater. Sci. Eng. 17 (2009) p. 025006.  
42  
43 [57] R.T. de Hoff, *Thermodynamics in Materials Science*, CRC Press, London, 2006.  
44  
45 [58] M. Sluiter, Comput. Mater. Sci. 2 (1994) p. 293.  
46  
47 [59] R. Meyer and P. Entel, Phys. Rev. B 57 (1998) p. 5140.  
48  
49 [60] G.J. Ackland, D.J. Bacon, A.F. Calder and T. Harry, Philos. Mag. A 75 (1997) p. 713.  
50  
51 [61] M. Ludwig, D. Farkas, D. Pedraza and S. Schmauder, Modelling Simul. Mater. Sci. Eng.  
52 6 (1998) p. 19.  
53  
54 [62] A. Caro, P.E.A. Turchi, M. Caro and E.M. Lopasso, J. Nucl. Mater. 336 (2005) p. 233.  
55  
56 [63] A. Caro, M. Caro, E.M. Lopasso, P.E.A. Turchi and D. Farkas, J. Nucl. Mater. 349  
57 (2006) p. 317.  
58  
59 [64] G. Salje and M. Feller-Kniepmeier, J. Appl. Phys. 48 (1977) p. 1833.  
60

- [65] M. Perez, F. Perrard, V. Massardier, X. Kleber, A. Deschamps, H. de Monestrol, P. Pareige and G. Covarel, *Phil. Mag.* 85 (2005) p. 2197.
- [66] N. Saunders and A.P. Miodownik, *CALPHAD (Calculation of Phase Diagrams): A Comprehensive Guide*, Pergamon, Oxford, 1998.
- [67] T.P.C. Klaver, R. Drautz and M.W. Finnis, *Phys. Rev. B* 74 (2006) p. 094435.
- [68] P. Erhart, B. Sadigh and A. Caro, *Appl. Phys. Lett.* 92 (2008) p. 141904.
- [69] I. Mirebeau, M. Hennion and G. Parette, *Phys. Rev. Lett.* 53 (1984) p. 687.
- [70] G. Bonny, R.C. Pasianot and L. Malerba, *Philos. Mag.* 89 (2009) p. 711.
- [71] A. van de Walle and G. Ceder, *Rev. Mod. Phys.* 74 (2002) p. 11.
- [72] M.J.D. Powell *Comput. J.* 7 (1965) 303-7.

### Figure caption

**Figure 1** - Overall view of the formation energies of low energy compounds.

**Figure 2** - Fe-rich phase boundary of the Fe-Cu system.

**Figure 3** - Phase diagram of the Cu-Ni system.

### Figures

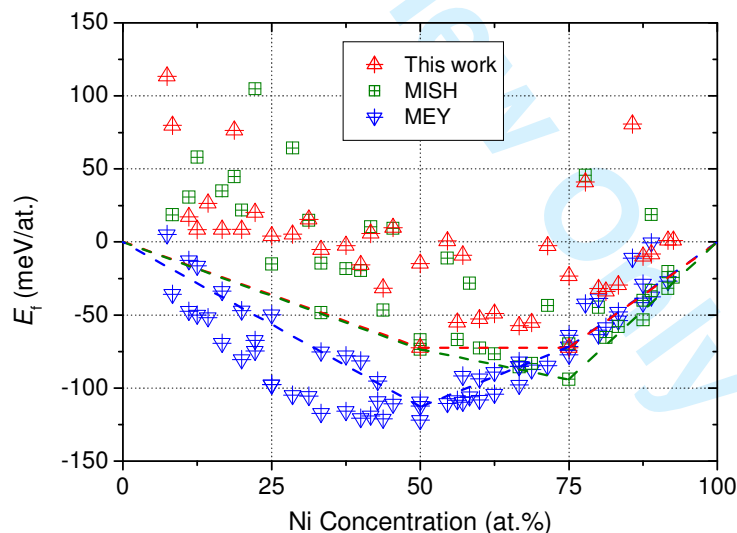


**Figure 1**

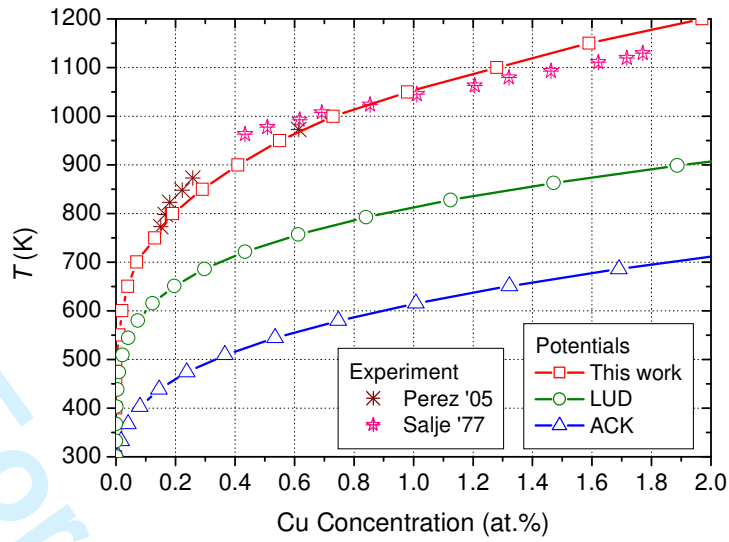


Figure 2

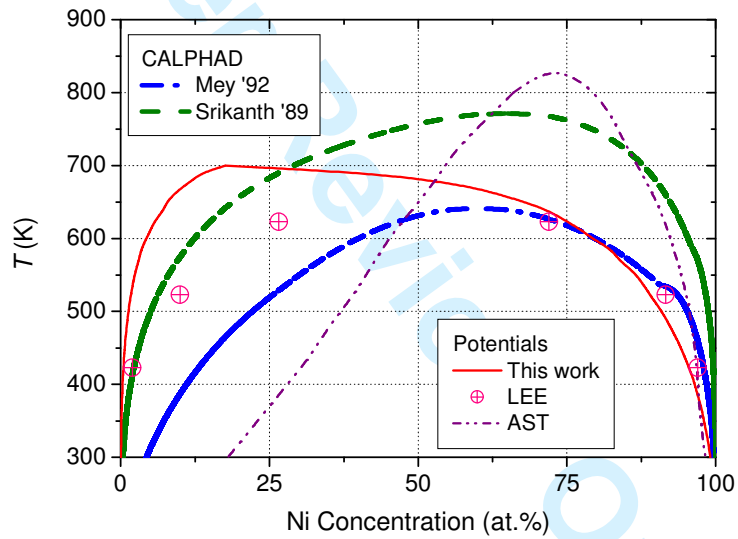
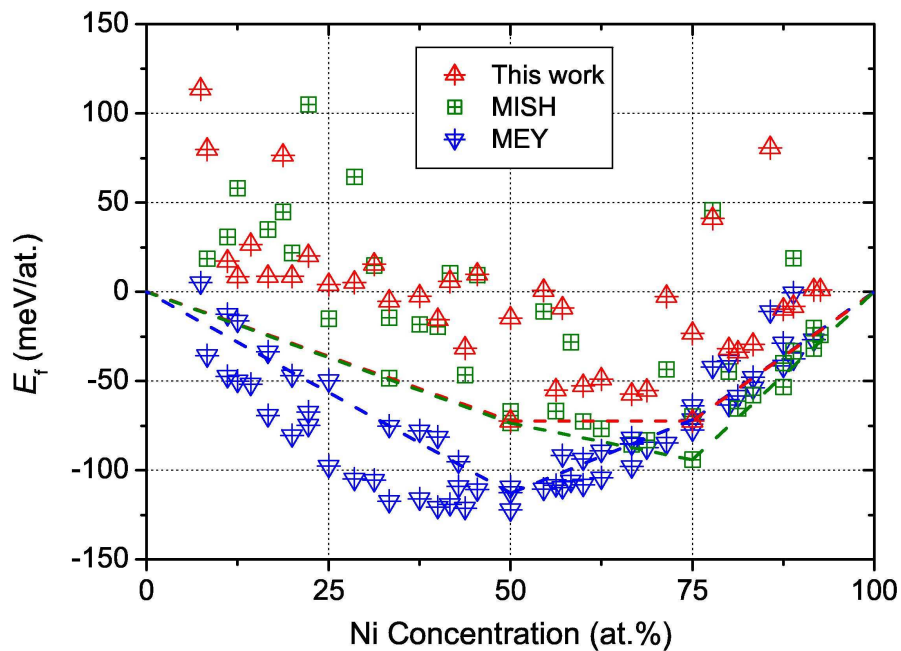
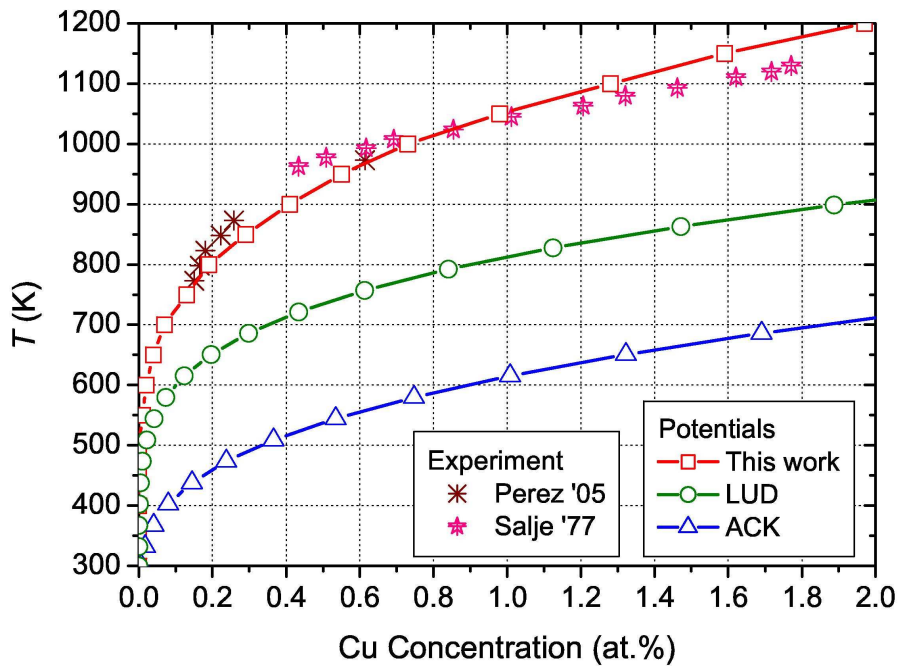


Figure 3



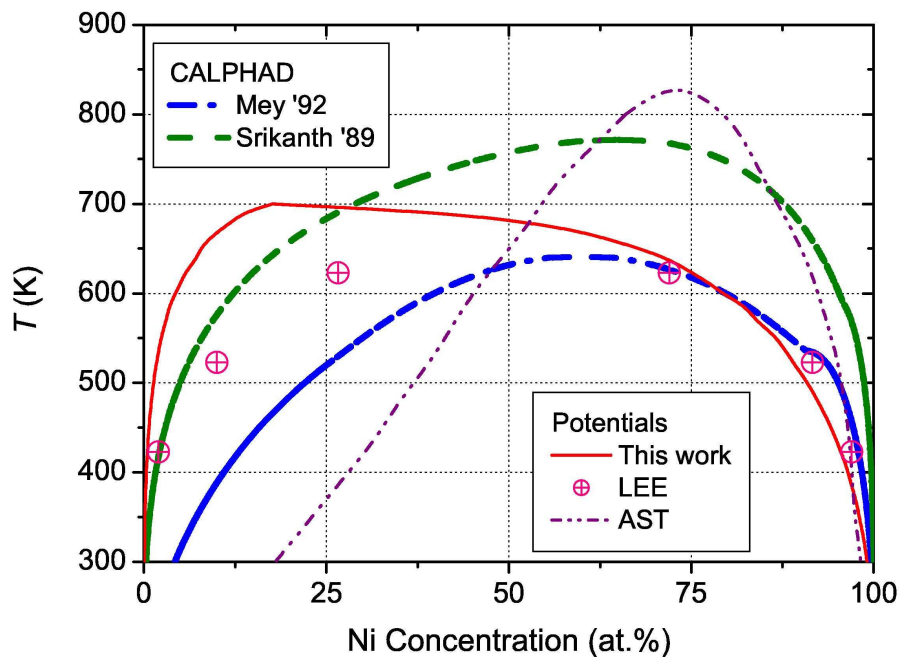
108x82mm (600 x 600 DPI)

View Only



106x82mm (600 x 600 DPI)

Manuscript Only



107x82mm (600 x 600 DPI)

Pre-proof Only